OBSERVATION OF WATER VAPOR WITH A PORTABLE RAMAN LIDAR --- CONTINUOUS MONITORING AND FIELD EXPERIMENTS OVER THE FOREST AND AT THE VOLCANO------

Takuji Nakamura[(1)], Naohiro Sugimoto[(1)], Toshitaka Tsuda[(1)] , Makoto Abo[(2)], Takeshi Hashimoto[(3)], Akihiko Terada[(3)(4)]

[(1)] RISH, Kyoto University, Uji, Kyoto 611-0011, Japan, E-mail:nakamura@rish.kyoto-u.ac.jp
[(2)] Graduate School of Electrical Engineering, Tokyo Metropolitan Univ., Hachioji,Tokyo, Japan , E-mail:abo@eei.metro-u.ac.jp
[(3)] Graduate School of Science, Hokkaido Univ., Sapporo, Japan, E-mail:hasimoto@uvo.sci.hokudai.ac.jp
[(4)] Now at, Graduate School of Science, Kyoto Univ., Japan, E-mail:terada@aso.vgs.kyoto-u.ac.jp

ABSTRACT

A transportable Raman lidar with a pulsed Nd:YAG laser (SHG(Second harmonic generation):532 nm) and a telescope with a 35.5 cm diameter has been built in order to monitor the water vapor profile in the boundary layer for day and night continuously, as well as up to the lower troposphere in the night time. The daytime measurement precision of specific humidity was about 10 – 20 % at 200 m altitude. Comparisons with local radiosondes at Shigaraki, Japan showed that calibration coefficient between the Raman channels was stable for over 6 months. This lidar has been applied to field observations of horizontal distribution of water vapor over the forest and in the volcanic gases utilizing the portability.

1. INTRODUCTION

Measurement or profiling of the atmospheric humidity, or water vapor content is of great value not only for meteorology but also various geophysical aspects, such as environmental change and green house effect, interaction between forest and atmosphere, as well as volcanological studies. As a profiling technique of humidity, lidar has been applied with two different approaches: Raman lidar and DIAL (DIfferential Absorption Lidar). The Raman lidar utilizes the fact that the wavelength of the scattered light is Raman shifted when the vibrational-rotational energy states of scatter molecules are changed. Although the different molecules could be discriminated by wavelengths and detection of waver vapor becomes possible, the very weak backscatter coefficient needs to have the sensitivity of the lidar large enough, and as a result Raman lidar system is likely to be a big system.

As one of the techniques of the water vapor profiling, RISH, Kyoto University has been developing a method using an VHF/UHF atmospheric radar [1]. From the information of scattering echo intensity, humidity profile could be derived. However, this technique requires a reference humidity value at some altitude to derive the profile from radar observation [2]. Therefore, we have developed a small Raman lidar for water vapor measurement by limiting the observation height range to a lower level of the boundary layer, which could be combined with radar observations. This paper is devoted to the introduction of this lidar system and its application to the observation of horizontal distribution of water vapor in a various fields.

2. SYSTEM DESIGN

The basic system diagram and outlook are shown in Fig. 1 and Fig. 2, respectively. The SHG output of a Nd:YAG laser with 30 mJ x 20 Hz output at 532 nm with a beam expander (5X) yielding 1.6 mrad beam divergence is used for transmission, and a Schmidt-Cassegrain telescope of 35.5 cm diameter (f = 3910mm) is equipped as a receiving telescope. The received lights are separated into three channels of elastic (532nm), N2 Raman (607 nm) and H20 Raman (660 nm) signals, using two dichroic beam splitters and interference filters. The detectors are PMT photon counting heads of Hamamatsu (H7360-01 for 532nm, and H7360-03 for other channels). The bandwidth of the interference filters of individual channels are 1.5 nm, 0.99 nm and 0.90 nm for 532 nm, 607nm and 660 nm, respectively.

The signals of 532 nm and 607 nm are attenuated by optical densities of 5 and 1, respectively, with ND filters, in order to avoid saturation in photon counting at the nearest range. After converted in to TTL level pulses, received signals are counted by a multi-channel scaler (AMCS-USB of Sigmaspace Corp.). The blocking of 532 nm signal at 607 nm and 660 nm are 10^6, and >10^10, respectively, and by a recent upgrade the former also now has become >10^10. The laser and

the multi-channel scaler are controlled by a PC with an operating system of Windows 2000 (SP4). A network power controller is used to reboot the photon counter (multi-channel scaler), and the PC and the network power controller are connected to the internet through a router.

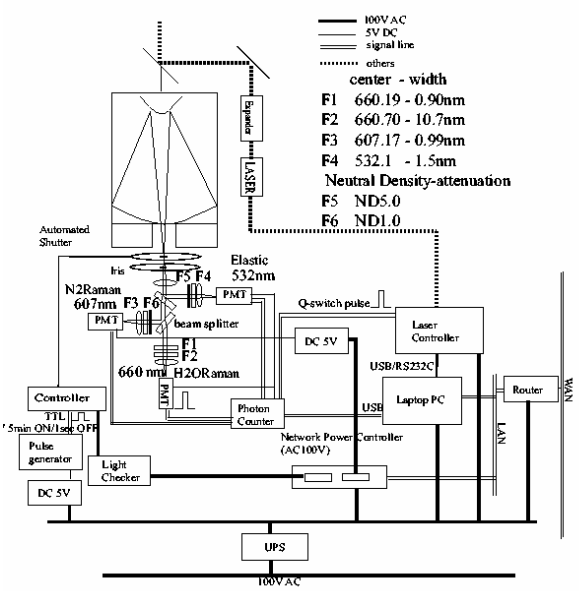

Fig. 1 System diagram of a portable Raman lidar

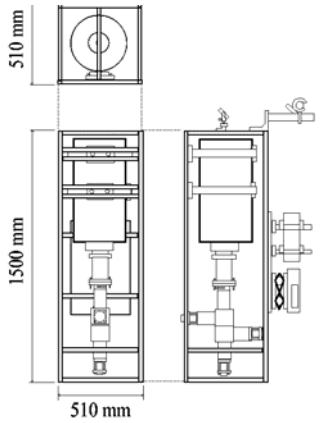

Fig. 2 Outlook of the system

3. HUMIDITY PROFILING OBSERVATIONS

The lidar is used to obtaining vertical profiles of water vapor mixing ratio. For day-and-night (24 hour) continuous observation, it was operated with 1.6 mrad beam divergence and FOV was set to 0.25 mrad in order to minimize the daylight background noise. The typical observation precision at 200 m altitude was 10-20 % and 12-35 % in June and December, 2004, respectively. In the night time they are improved up to 2-6 % and 1 - 7 %, respectively, and at 600 m height, 14-22 % and 18-32 %, respectively. The precision of daytime measurement was significantly improved using a narrower beam diveregence (0.2 mrad) by a factor of 5 or more below 300 m. However above that the precision becomes worse probably because of the effect of the secondary mirror.

The humidity profiles are calibrated with local radiosondes. Fig. 3 shows comparison between specific humidity observed by radiosonde (red) and lidar (black). The calibration was carried out for the data of Nov 5-6, 2004. There is not a significant bias, and the calibration coefficient could be used for more than 6 months.

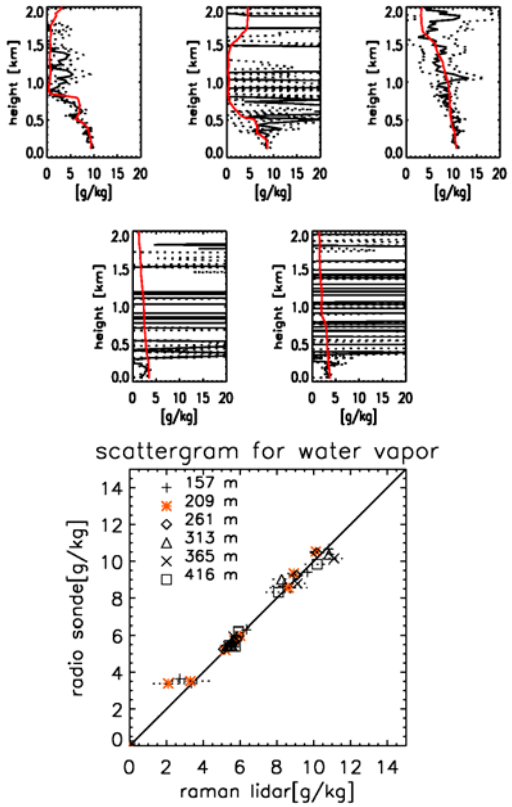

Fig. 3 Comparison of specific humidity by radiosonde and lidar. (Top left) 0400 LT of May 12, 2004. (Top middle) 0900 LT. (Top right) 0100 of May 13, 2004. (Center left) 1400 LT of March 25, 2005. (Center right) 1600 LT. (Bottom) Scatter diagram of measurements between lidar and radiosonde.

Fig. 4 shows an example of one week observations as a time-height cross section of humidity (top) and backscatter ratio (middle), together with the comparison with the surface data (bottom) with 30 min resolution. In the daytime, observation altitude is limited to 400 m due to strong sky background, but in the nighttime observation could be done up to 1 km. Increase of humidity and aerosols can be seen in the plot.

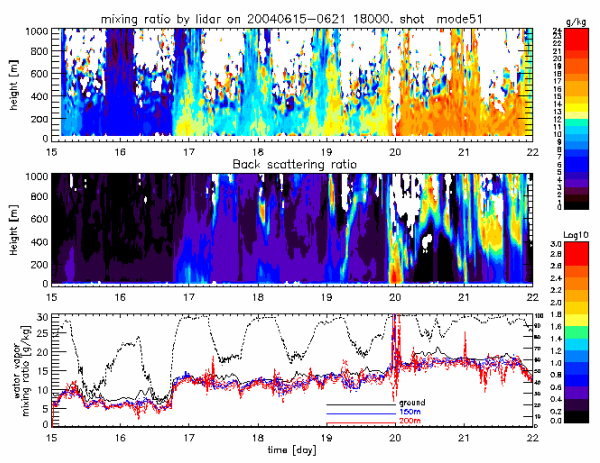

Fig. 4 Water vapor mixing ratio (top), backscatter ratio (middle) and comparison with the surface weather data (bottom). The surface data includes relative humidity (dotted) and specific humidity (solid). Red and blue lines are specific humidity at 200 m and 150 m altitudes, respectively.

In case of nighttime observation without daytime operation, the iris is set to allow larger FOV (3.8 mrad) and therefore sensitivity is improved. Humidity profiles could be obtained up to 3-4 km, although depending on the season and atmospheric conditions. In case of nighttime observation, signal induced noise could be detected. This could be due to the florescence of the window of the room in front of the system. However, the effect of signal induced noise could be removed using a linear fitting to the log-signal intensity between 5 and 10 km range, which has been confirmed with the simultaneous radiosonde data.

4. HORIZONTAL DISTRIBUTION OF WATER VAPOR OVER THE NATIONAL FOREST AT SHIGARAKI

Horizontal distribution of the humidity (water vapor mixing ratio) and backscatter ratio was observed over the forest around Shigaraki MU observatory (136.1E, 34.9N, 370 m above sea level). The lidar is located horizontally at the 2nd floor of the MU radar observatory with the window opened. In the nighttime, FOV was set to be 3.8 mrad, whereas in the daytime, FOV was about one order of magnitude smaller to decrease the background light. Fig. 4 shows the relation of the line of sight and the topography of the national forest. The beam pointing direction was about 0.7 degree below the horizon. The lidar samples atmosphere observed up to 4 km in distance, where the beam hit the mountain surface. The maximum height from the ground was about 150 m at around 2 km in distance.

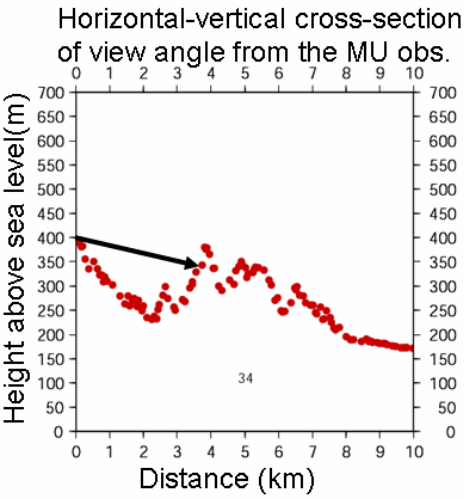

Fig. 5. Line-of-sight direction for the horizontal observation with the portable lidar at Shigaraki MU radar observatory.

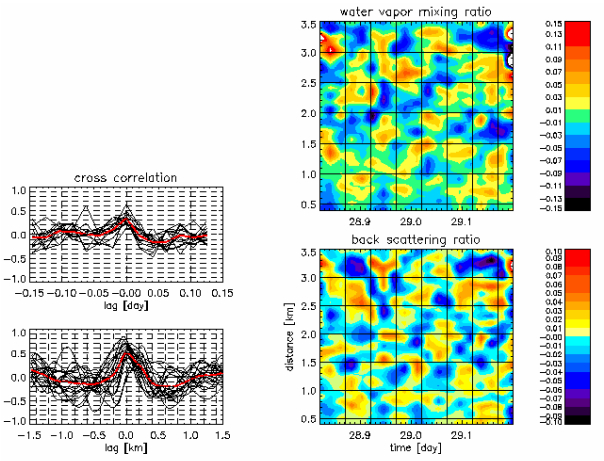

Fig. 6. Fluctuation of water vapor mixing ratio (top right) and backscatter ratio (bottom right) observed on August 28-29, 2005. See the text.

The result in the night time at 19:00 – 29:00 LT on August 28, 2005 is presented on Fig. 6. For this observation period random error at 500 m, 2 km and 3.5 km was 2%, 6%, and 10%, respectively, with 30 min integration and 60 m, 240 m and 480 m averaging, respectively. The obtained data were subject to correction of overlapping function between the channels and then a normalization using the H20/N2 Raman ratio of 0.5 – 1.5 km. Then a band-pass filter with cut-off length of 200 – 2000 m was applied in order to pickup the fluctuating component in space. The right top panel in Fig. 6 shows derived water vapor fluctuation. The amplitude of the spatial and temporal variation of water vapor reached about 10 % with typical scale of 500 – 1000 m and 1-2 hours. The right bottom panel displays the time-range variation of backscatter ratio, after the same filtering process. Correlation coefficient in

temporal (bottom left) and spatial (bottom right) lags are also plotted. The time-range fluctuations of water vapor and backscatter ratio shown in the right panels are very similar. From the cross correlation functions both variations are found to be in phase. The vertical displacement of the air parcel of the observed horizontal and time scales could be due to such large fluctuation of the humidity.

5. OBSERVATION OF WATER VAPOR IN THE VOLCANIC GAS AT MT. ASO

The water vapor in the volcanic gas is a very important source of energy flux from underground to the atmosphere. Nevertheless, the measurement of water vapor content in the volcanic gas has not been successfully done. In this study, we tried a measurement of the volcanic gas at Nakadake, Mt. Aso by transporting the lidar to the crater side. The lidar was equipped horizontally in the vehicle and laser beam was nearly horizontally emitted. By changing the direction of the car, water vapor and backscatter ratio distribution in the two directions, one toward the volcanic gas and the other deviated from it, were measured as a function of distance. The location and direction is shown in Fig. 7.

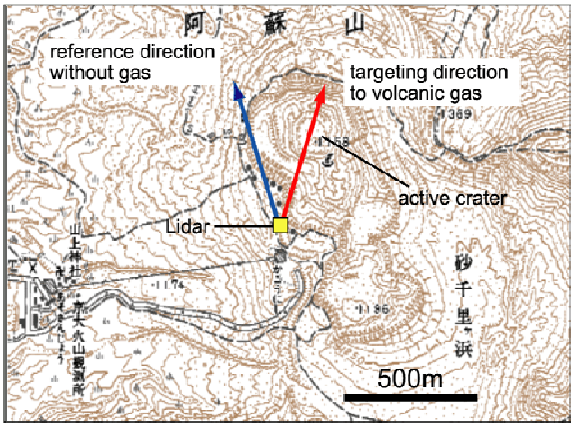

Fig. 7. Map of the observation point and directions of lidar on November 23, 2005 at Mt. Aso.

Fig. 8 shows the backscatter ratio distribution for the volcanic fumarole and reference air, showing the distance to the center of the gas column is at about 500 m and the width was 300 m. The distribution of waver vapor mixing ratio for both directions is indicated in Fig. 9. It should be noted that the effect of wavelength dependence of extinction was not considered in Fig. 9. Therefore, the water vapor at 300-400 m or more could be biased with this effect. We, however, estimated that the water vapor in the volcanic gas was about 0.4 g/kg larger than the reference direction (background). The detailed discussion and estimation of waver vapor flux is still undergoing, but we can conclude that a portable Raman lidar is capable of measuring water vapor distribution in the volcanic gas, much more directly than the previous studies [3].

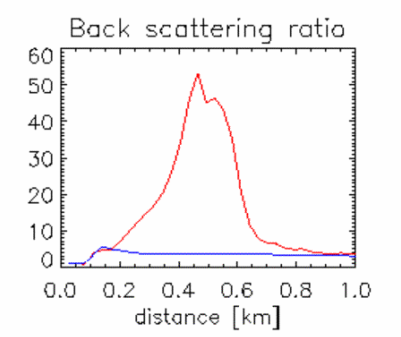

Fig. 8. Distribution of backscatter ratio observed at Mr. Aso. Red and blue lines correspond to directions to volcanic gas and background atmosphere, respectively.

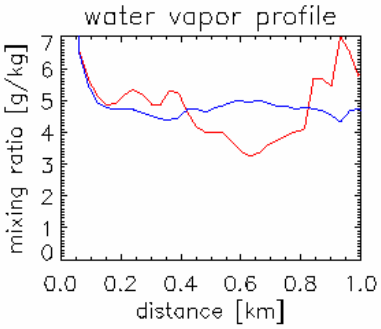

Fig. 9 The same as Fig. 8, except for the water vapor mixing ratio. See the text.

6 References

1. Tsuda T., et al., Estimation of a Humidity Profile Using Turbulence Echo Characteristics, *J. Atmos. Oceanic Technol.*, Vol. 18, 1213-1222, 2001.

2. Furumoto J.-I, et al., Estimation of Humidity Profiles with the L-band Boundary Layer Radar-RASS Measurement, *J. Meteor. Soc. J.*, Vol. 82, 895 – 908, 2005.

3. Kagiyama, T., Evaluation methods of heat discharge and their applications to the major active volcanoes in Japan, *J. Volcanol. Geotherm. Res.*, 9, 87-97, 1981.